Eur. Phys. J. A **24**, 51–56 (2005)
DOI 10.1140/epja/i2004-10122-9

THE EUROPEAN PHYSICAL JOURNAL A

A search for spontaneous emission of heavy clusters in the ^{127}I nuclide

R. Bernabei[1,a], P. Belli[1], F. Cappella[1], F. Montecchia[1,b], F. Nozzoli[1], A. d'Angelo[2,c], A. Incicchitti[2], D. Prosperi[2], R. Cerulli[3], C.J. Dai[4], H.L. He[4], H.H. Kuang[4], J.M. Ma[4], Z.P. Ye[4,d], and V.I. Tretyak[5]

[1] Dipartimento di Fisica, Università di Roma "Tor Vergata" and INFN, Sezione di Roma2, I-00133 Roma, Italy
[2] Dipartimento di Fisica, Università di Roma "La Sapienza" and INFN, Sezione di Roma, I-00185 Roma, Italy
[3] INFN - Laboratori Nazionali del Gran Sasso, I-67010 Assergi (AQ), Italy
[4] IHEP, Chinese Academy, P.O. Box 918/3, Beijing 100049, PRC
[5] Institute for Nuclear Research, MSP 03680 Kiev, Ukraine

Received: 26 October 2004 / Revised version: 5 January 2005 /
Published online: 27 January 2005 –
Communicated by P. Picozza

Abstract. The results of an experimental search for spontaneous cluster decay in ^{127}I are presented. Several possible channels have been investigated considering an exposure of 33834 kg · day collected by a large-mass highly radiopure NaI(Tl) set-up deep underground in the Gran Sasso National Laboratory of the INFN. New lower limits on the lifetime of $^{24}_{10}$Ne, $^{28}_{12}$Mg, $^{30}_{12}$Mg, $^{32}_{14}$Si, $^{34}_{14}$Si, $^{48}_{20}$Ca, $^{49}_{21}$Sc cluster radioactivity in ^{127}I have been achieved.

PACS. 21.65.+f Nuclear matter – 27.60.+j $90 \leq A \leq 149$ – 23.60.+e α decay – 29.40.Mc Scintillation detectors

1 Introduction

The spontaneous emission of nuclear fragments heavier than α particles and lighter than the most probable fission fragments, named cluster decay, was theoretically predicted in 1980 [1] and experimentally observed for the first time in 1984 [2,3]. Up to date, spontaneous emission of clusters ranging from ^{14}C to ^{34}Si from near twenty translead nuclei (from ^{221}Fr to ^{242}Cm) have been observed with branching ratios relative to α-decay from 10^{-9} down to 10^{-16} and partial half-lives from 3.2×10^3 y up to 1.2×10^{20} y [4,5]. In all these decays, double magic nucleus ^{208}Pb, or nuclei close to ^{208}Pb, are produced; for this reason this effect has been cited in literature as "lead radioactivity" [5]. For about ten cases, only the half-life limits are known with the highest value of $T_{1/2} > 5.0\times10^{21}$ y for decay $^{232}\text{Th} \rightarrow {}^{24-26}\text{Ne} + {}^{208-206}\text{Hg}$ [4,6].

A new region of parent nuclei, for which cluster radioactivity can be observed experimentally, was predicted recently in ref. [7]: these are the nuclei with $Z = 56$–64 and $N = 58$–72; daughter nuclei are close to double magic $^{100}_{50}$Sn. First searches in this domain were performed resulting only in limit $T_{1/2} > 3.5$ h for $^{114}\text{Ba} \rightarrow {}^{12}\text{C} + {}^{102}\text{Sn}$ [8].

In the present experiment, possible cluster decays of ^{127}I have been investigated. Using a new table of atomic masses [9], one can find that 215 different decay modes are possible for this nucleus with positive-energy release Q. However, probably the most interesting ones are those with emission of double magic nucleus $^{48}_{20}$Ca and its neighbour $^{49}_{21}$Sc: they have the highest Q values of 28.9 and 29.4 MeV, respectively [9]. Other examples, investigated in this work, lie in the region close to $^{100}_{50}$Sn.

Theoretical calculations for ^{127}I cluster decay, based on analytical superasymmetric fission model [10], were pessimistic: estimated half-lives were greater than 10^{43} y. Recently, several semiempirical formulae for the calculation of $T_{1/2}$ in cluster decays were proposed [11–13] with numerical parameters determined by fitting the known experimental data. However, despite these formulae work nicely in the region of the so-called "lead radioactivity" [5], they give very discrepant results when applied to cluster decay of ^{127}I: calculated $T_{1/2}$ differ by orders of magnitude. In case of $^{48}_{20}$Ca and $^{49}_{21}$Sc emission, the model [12] gives unrealistically low ^{127}I half-lives of 1.6×10^6 y and 2.1 h, respectively. Such a discrepancy gives us additional

[a] e-mail: rita.bernabei@roma2.infn.it
[b] Also at: Università "Campus Bio-Medico" di Roma, 00155, Roma, Italy.
[c] Also at: Scuola di Specializzazione in FISICA SANITARIA, Università di Roma "Tor Vergata", I-00133 Roma, Italy.
[d] Also at: University of Zhao Qing, Guang Dong, PRC.

motivation for experimental investigation of the ^{127}I cluster decay.

The most widely used technique in experiments on cluster radioactivity is based on solid-state nuclear track detectors which are able to register the tracks of the heavy clusters emitted from thin samples while rejecting much more numerous low-energy α particles with great efficiency [4]. In few first measurements also Si detector telescopes were applied [2]. Ge detectors were used in two experiments looking for γ-rays created in cluster decay nuclear residuals: ^{24}Na in the decay of ^{233}U (where the limit $T_{1/2} > 1.7 \times 10^{17}$ y was established) [14], and various clusters in decays of Hg isotopes (with $T_{1/2}$ limits up to few by 10^{21} y) [15]. In our research the ^{127}I parent nuclei are incorporated in the NaI detector itself (natural abundance of ^{127}I is 100%) and the initial energy release and the subsequent decay of the created clusters (which usually are radioactive) are searched for.

The present search has been carried out by using data collected deep underground (about 3600 m.w.e.) at the Gran Sasso National Laboratory of INFN by using the highly radiopure $\simeq$ 100 kg NaI(Tl) set-up of the DAMA experiment (DAMA/NaI). This set-up has been mainly devoted to the investigation of Dark-Matter particle in the galactic halo exploiting the annual modulation signature [16–18], but has also investigated other approaches and several rare processes [19,20]. In particular, in ref. [19] data collected in the tens MeV energy region have already been used to investigate possible spontaneous emission of protons due to violation of the Pauli exclusion principle. DAMA/NaI has completed its data taking in July 2002 and has been replaced by DAMA/LIBRA ($\simeq$ 250 kg highly radiopure NaI(Tl)), now running.

The processes investigated in the present experimental search are: i) $^{127}_{53}\mathrm{I} \to {}^{30}_{12}\mathrm{Mg} + {}^{97}_{41}\mathrm{Nb}$; ii) $^{127}_{53}\mathrm{I} \to {}^{34}_{14}\mathrm{Si} + {}^{93}_{39}\mathrm{Y}$; iii) $^{127}_{53}\mathrm{I} \to {}^{24}_{10}\mathrm{Ne} + {}^{103}_{43}\mathrm{Tc}$; iv) $^{127}_{53}\mathrm{I} \to {}^{28}_{12}\mathrm{Mg} + {}^{99}_{41}\mathrm{Nb}$; v) $^{127}_{53}\mathrm{I} \to {}^{32}_{14}\mathrm{Si} + {}^{95}_{39}\mathrm{Y}$; vi) $^{127}_{53}\mathrm{I} \to {}^{49}_{21}\mathrm{Sc} + {}^{78}_{32}\mathrm{Ge}$; vii) $^{127}_{53}\mathrm{I} \to {}^{48}_{20}\mathrm{Ca} + {}^{79}_{33}\mathrm{As}$. The deep experimental site, the large exposure, the effective shielding of the detectors and the detectors' radiopurity have allowed to investigate these possible processes by using NaI(Tl) crystals.

2 Experimental results

The description of the set-up and of its main performances have been given in ref. [21]: moreover, some other information on its performances and on the upgrading occurred in 2000 have been given in refs. [17,18]. We only remind that the data considered here have been collected with nine 9.70 kg highly radiopure NaI(Tl) crystal scintillators (3 columns of 3 detectors each one) enclosed in suitably radiopure Cu housings. Each detector has two 10 cm long tetrasil-B light guides directly coupled to the opposite sides of the bare crystal; two low background photomultipliers work in coincidence. The detectors are enclosed in a low radioactive copper box inside a low radioactive shield made by 10 cm copper and 15 cm lead. The lead is surrounded by 1.5 mm Cd foils and about 10/40 cm of polyethylene/paraffin; moreover, the installation is almost completely surrounded by about 1 m of concrete acting as a further neutron moderator. A high-purity (HP) nitrogen atmosphere is maintained inside the copper box. The passive shield is also enclosed in a sealed plexiglas box maintained in HP nitrogen atmosphere as well as the glove-box which is located on the top of the shield to allow the detectors calibration in the same running conditions without any contact with the external environment. The installation is subjected to air conditioning. As of interest here, the energy, the identification of the fired crystals and the absolute time occurrence are acquired for each event. The calibration has been performed with several gamma sources; the energy resolution in the high-energy region is typically $\frac{\sigma}{E} = \frac{0.0104}{\sqrt{E(\mathrm{MeV})}} + 0.0324$.

The data analysis has been performed by searching in an exposure of 33834 kg $\cdot$ day for peculiar events according to the procedures described in the following subsections. In particular, such possible decays have been investigated by searching for the energy released in the initial decay (detected energy depends on the Q value and on the light yields of the nuclear fragments) and subsequent decays of radioactive daughter nuclei. In those cases when the initial or intermediate decay has too long lifetime, only subsequent decays of radioactive daughter nuclei have been looked for. In particular, in order to reduce at most the background contribution, very selective event patterns have been considered; consequently, they select small fractions of the total ^{127}I cluster decay in the studied channels. However, limits of the same orders of magnitude as those presented in the following can be achieved when considering some other peculiar components of the decays.

2.1 The channel $^{127}_{53}\mathrm{I} \to {}^{30}_{12}\mathrm{Mg} + {}^{97}_{41}\mathrm{Nb}$

Figure 1 shows the most relevant part of the decay chain of the $^{30}_{12}$Mg produced in a possible $^{127}_{53}\mathrm{I} \to {}^{30}_{12}\mathrm{Mg} + {}^{97}_{41}\mathrm{Nb}$ spontaneous cluster decay. In the following, we exploit only the features of this more selective decay chain since the $^{97}_{41}$Nb has a longer half-life (72.1 m).

In this way, a clean pattern can be obtained for the cluster decay mode searched for. In particular, for each detector, a, we have searched for an event pattern with the following time sequence: i) occurrence of an event with multiplicity $M = 1$ (only the detector a fires) and energy E_{a_1} released by the $^{30}_{12}$Mg and the $^{97}_{41}$Nb fragment nuclei; ii) occurrence —after a time delay Δt_1— of an event with $M = 2$ involving the detector a and an adjacent one, b (energies E_{a_2} and E_{b_2}, respectively), induced by the $^{30}_{12}$Mg β-decay (mainly β in the detector a and an associated γ in the detector b); iii) occurrence —after a time delay Δt_2— of another event with $M = 2$ involving the detector a and an adjacent one, c[1] (energies E_{a_3} and E_{c_3}, respectively), induced by the $^{30}_{13}$Al β-decay (mainly β in the detector a and an associated γ in the detector c).

[1] c may also be equal to b.

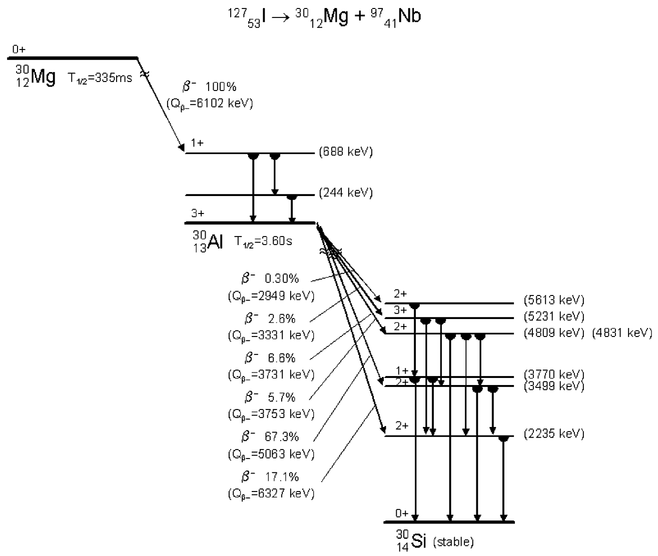

Fig. 1. Main part of the decay chain useful to understand the event pattern considered here to investigate the $^{127}_{53}\mathrm{I} \to ^{30}_{12}\mathrm{Mg} + ^{97}_{41}\mathrm{Nb}$ cluster decay [22]. The Monte Carlo simulation for the efficiency evaluation obviously accounts for the whole decay schema of all the involved isotopes.

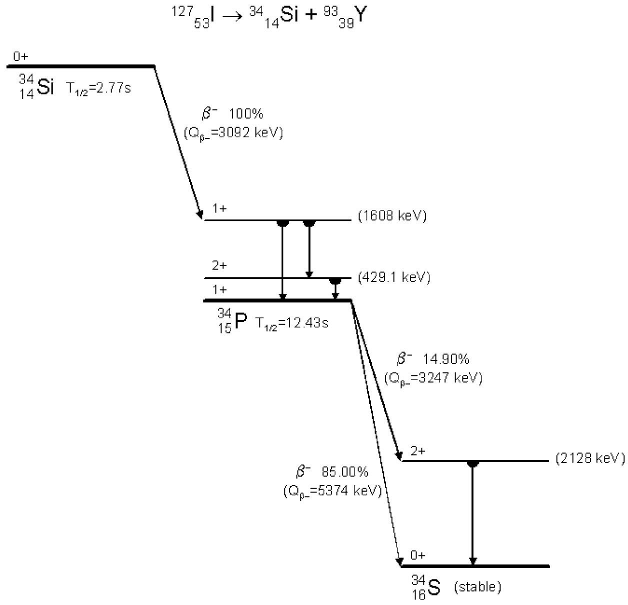

Fig. 2. Main part of the decay chain useful to understand the event pattern considered here to investigate the $^{127}_{53}\mathrm{I} \to ^{34}_{14}\mathrm{Si} + ^{93}_{39}\mathrm{Y}$ cluster decay [22]. The Monte Carlo simulation for the efficiency evaluation obviously accounts for the whole decay schema of all the involved isotopes.

In the analysis of the experimental data the acceptance energy window for E_{a_1} has been chosen large enough to account for the unavoidable uncertainties on the quenching factors of the nuclear fragments. In particular, it has been taken equal to 1 MeV $< E_{a_1} <$ 2 MeV, considering that the Q value of the process is 5.5 MeV and that, if assuming for template purpose a quenching factor equal to 0.3 for the lighter fragment and 0.09 for the heavier one (values measured for the used NaI(Tl) in case of ^{23}Na and ^{127}I recoils [23]), E_{a_1} would be equal to 1.4 MeV.

The restrictions on the other parameters have been suitably derived from the $^{30}_{12}$Mg decay scheme given in fig. 1 and are: i) $\Delta t_1 < 1$ s; ii) $\Delta t_1 + \Delta t_2 < 12$ s; iii) E_{a_2} and E_{a_3} greater than 2 MeV; iv) $E_{b_2} > 0.2$ MeV and $E_{c_3} > 1.0$ MeV. These restrictions allow to select 1.3% of the total ^{127}I cluster decay in the studied channel as evaluated by the Monte Carlo code (based on EGS4 [24]), which accounts for the geometry and the performances of the experimental set-up and for the studied process.

Zero events with the features searched for have been found in the analysed exposure; this number gives rise —for the whole exposure— to a 90% C.L. upper limit [25] on the cluster decays of the searched mode (S) of 177. Thus, from the known formula

$$\tau = \frac{N_I \cdot M \cdot T}{S} ,$$

being $N_I = 4.015 \times 10^{24}$ iodine nuclei per kg of NaI(Tl) and $M \cdot T = 33834$ kg · day, one gets, for the lifetime of the process,

$$\tau(^{127}_{53}\mathrm{I} \to ^{30}_{12}\mathrm{Mg} + ^{97}_{41}\mathrm{Nb}) > 2.1 \times 10^{24} \;\; \mathrm{y} \quad (90\% \text{ C.L.}).$$

2.2 The channel $^{127}_{53}\mathrm{I} \to ^{34}_{14}\mathrm{Si} + ^{93}_{39}\mathrm{Y}$

Figure 2 shows the most relevant part of the decay chain of the $^{34}_{14}$Si produced in a possible $^{127}_{53}\mathrm{I} \to ^{34}_{14}\mathrm{Si} + ^{93}_{39}\mathrm{Y}$ spontaneous cluster decay. In the following we exploit only the features of this more selective decay chain, since the $^{93}_{39}$Y has a longer half-life (10.18 h). Also in this case, a clean pattern for the cluster decay mode searched for can be exploited.

In particular, for each detector we have searched for an event pattern equal to that of the previous case, but of course with different restrictions on the parameters. In this case, the first event is given by the $^{34}_{14}$Si and the $^{93}_{39}$Y energy releases, the second and the third are instead induced by the β-decay of $^{34}_{14}$Si and $^{34}_{15}$P, respectively (β's in the detector a and associated γ's in the detector b or c, respectively).

On the basis of considerations similar to those given in the previous subsection (here the Q value is 15.2 MeV), for safety in the data analysis we consider the broad energy region: $3.0 < E_{a_1} < 4.5$ MeV. The other restrictions are: i) $\Delta t_1 < 10$ s; ii) $\Delta t_1 + \Delta t_2 < 30$ s; iii) E_{a_2} and E_{a_3} greater than 1.0 MeV; iv) $E_{b_2} > 1.0$ MeV and E_{c_3} in the $\pm 2\sigma$ energy window around 2.13 MeV (see fig. 2). These restrictions allow to select 3.4×10^{-4} of the total ^{127}I cluster decay in the studied channel as evaluated by the Monte Carlo code.

Zero events with the features searched for have been found in the analysed exposure for this possible decay channel, giving $S < 6765$ cluster decays at 90% C.L.; thus

$$\tau(^{127}_{53}\mathrm{I} \to ^{34}_{14}\mathrm{Si} + ^{93}_{39}\mathrm{Y}) > 5.5 \times 10^{22} \;\; \mathrm{y} \quad (90\% \text{ C.L.}).$$

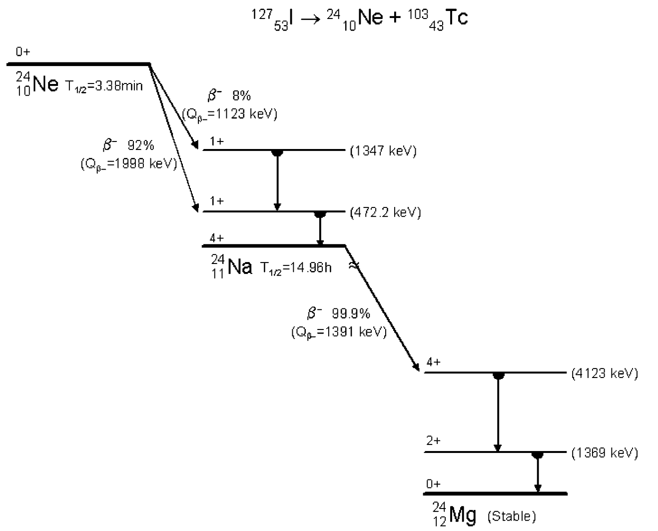

Fig. 3. Main part of the decay chain useful to understand the event pattern considered here to investigate the $^{127}_{53}\mathrm{I} \to {}^{24}_{10}\mathrm{Ne} + {}^{103}_{43}\mathrm{Tc}$ cluster decay [22]. The Monte Carlo simulation for the efficiency evaluation obviously accounts for the whole decay schema of all the involved isotopes.

2.3 The channel $^{127}_{53}\mathrm{I} \to {}^{24}_{10}\mathrm{Ne} + {}^{103}_{43}\mathrm{Tc}$

Figure 3 shows the most relevant part of the decay chain of the $^{24}_{10}\mathrm{Ne}$ produced in a possible $^{127}_{53}\mathrm{I} \to {}^{24}_{10}\mathrm{Ne} + {}^{103}_{43}\mathrm{Tc}$ spontaneous cluster decay. The $^{103}_{43}\mathrm{Tc}$ decay chain is not more selective offering only relatively low-energy γ's (mainly with energies below 0.6 MeV).

Thus, a clear pattern for such a decay mode is achieved by studying the presence of $^{24}\mathrm{Na}$ nuclide inside the NaI(Tl) crystals. In fact, as shown in fig. 3, the $^{24}\mathrm{Na}$ β-decays emitting two characteristic photons of 1.369 MeV and 2.754 MeV. Therefore, the presence of $^{24}\mathrm{Na}$ has been investigated by looking for events with $M = 3$ induced by a β with end-point at 1.4 MeV (E_1) in one detector and the two γ's in two adjacent ones (E_2, E_3). In particular, we consider: i) 0.2 MeV $< E_1 <$ 1.4 MeV, ii) E_2 and E_3 inside $\pm 1\sigma$ energy windows around the photopeak positions. With these restrictions the efficiency of the process evaluated by the Monte Carlo code is $2.5 \cdot 10^{-3}$ of the total $^{127}\mathrm{I}$ cluster decay in the studied channel.

Three events satisfying the requirements have been found; they can be ascribed to side processes. Safely we consider that the number of detected events from the decay mode searched for is lower than 6.68 (90% C.L.) following the procedure given in [25]; thus, $S < 2672$ cluster decays and

$$\tau(^{127}_{53}\mathrm{I} \to^{24}_{10}\mathrm{Ne} +^{103}_{43}\mathrm{Tc}) > 1.4 \times 10^{23}\ \mathrm{y} \quad (90\%\ \mathrm{C.L.}).$$

2.4 The channel $^{127}_{53}\mathrm{I} \to {}^{28}_{12}\mathrm{Mg} + {}^{99}_{41}\mathrm{Nb}$

Figure 4 shows the most relevant part of the decay chain of the $^{28}_{12}\mathrm{Mg}$ produced in a possible $^{127}_{53}\mathrm{I} \to {}^{28}_{12}\mathrm{Mg} + {}^{99}_{41}\mathrm{Nb}$ spontaneous cluster decay. The $^{99}_{41}\mathrm{Nb}$ decay chain is not more selective offering only relatively low-energy γ's (mainly with energies below 1 MeV).

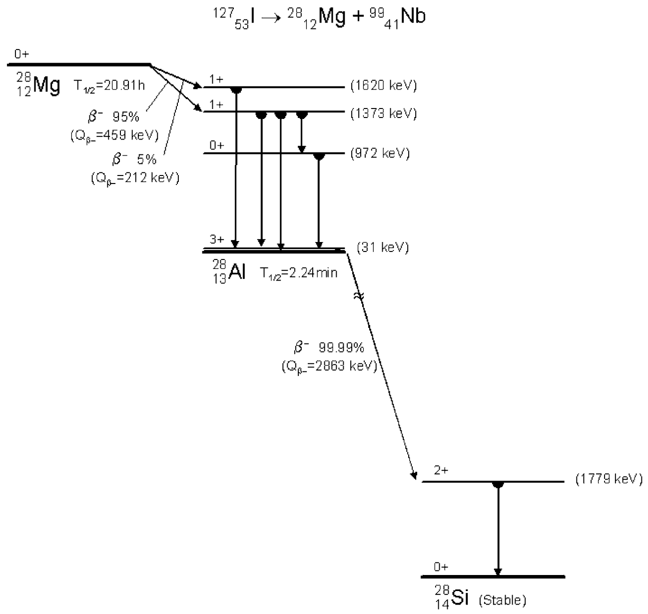

Fig. 4. Main part of the decay chain useful to understand the event pattern considered here to investigate the $^{127}_{53}\mathrm{I} \to {}^{28}_{12}\mathrm{Mg} + {}^{99}_{41}\mathrm{Nb}$ cluster decay [22]. The Monte Carlo simulation for the efficiency evaluation obviously accounts for the whole decay schema of all the involved isotopes.

In particular, for this considered cluster decay mode, for each detector a we have searched for an event pattern with the following time sequence: i) occurrence of an event with $M = 2$ involving the detector a and an adjacent one, b (energies E_{a_1} and E_{b_1}, respectively), induced by the $^{28}_{12}\mathrm{Mg}$ β-decay (mainly β in the detector a and associated γ's in the detector b); ii) occurrence after a time delay Δt_1 of another event with $M = 2$ involving the detector a and an adjacent one, c [2] (energies E_{a_2} and E_{c_2}, respectively), induced by the $^{28}_{13}\mathrm{Al}$ β-decay (mainly β in the detector a and an associated γ in the detector c).

The restrictions on the parameters have been suitably derived from the $^{28}_{12}\mathrm{Mg}$ decay scheme in fig. 4 and are: i) $\Delta t_1 < 200$ s; ii) 0.20 MeV $< E_{a_1} <$ 0.46 MeV; iii) E_{b_1} in the window: [1342 keV (energy of the first considered photon) -1σ]–[1373 keV (energy of the second considered photon) $+ 1\sigma$]; iv) 1.5 MeV $< E_{a_2} <$ 2.8 MeV; v) E_{c_2} inside a $\pm 1\sigma$ energy window around the 1.78 MeV photopeak position. These restrictions allow to select 2.7×10^{-4} of the total $^{127}\mathrm{I}$ cluster decay in the studied channel as evaluated by the Monte Carlo code.

Five events with the features searched for have been found in the analysed exposure; they can be ascribed to random coincidences whose expected number is (5.2±0.3). Following the procedure outlined in [25] for Poissonian events in the presence of a background with associated Gaussian uncertainty, a 90% C.L. upper limit on events from the searched decay mode of 5.08 events has been

[2] c may also be equal to b.

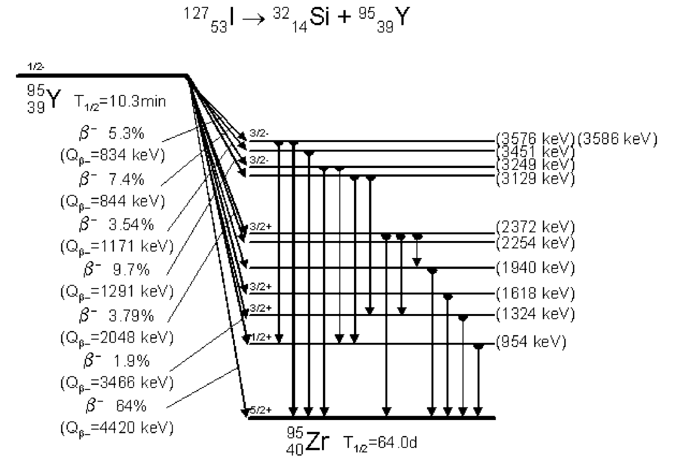

Fig. 5. Main part of the decay chain useful to understand the event pattern considered here to investigate the $^{127}_{53}$I $\rightarrow$ $^{32}_{14}$Si + $^{95}_{39}$Y cluster decay [26]. The Monte Carlo simulation for the efficiency evaluation obviously accounts for the whole decay schema of all the involved isotopes.

obtained. Therefore, $S < 1.9 \times 10^4$ cluster decays (90% C.L.) in the analysed exposure, leading to the restriction:

$$\tau(^{127}_{53}\mathrm{I} \rightarrow^{28}_{12}\mathrm{Mg} +^{99}_{41}\mathrm{Nb}) > 2.0 \times 10^{22} \ \ \mathrm{y} \quad (90\% \ \mathrm{C.L.}).$$

2.5 The channel $^{127}_{53}$I $\rightarrow$ $^{32}_{14}$Si + $^{95}_{39}$Y

Figure 5 shows the most relevant part of the decay chain of the $^{95}_{39}$Y produced in a possible $^{127}_{53}$I $\rightarrow$ $^{32}_{14}$Si + $^{95}_{39}$Y spontaneous cluster decay. In the following we exploit only some feature of this more selective decay chain since the $^{32}_{14}$Si has a long half-life (172 y).

A suitable pattern to investigate such a decay mode is achieved by studying the presence of ^{95}Y nuclide inside the NaI(Tl) crystals. In fact, as shown in fig. 5, the ^{95}Y β-decays emitting in 7% of the cases two characteristic photons of 0.954 MeV and 2.176 MeV. Therefore, the presence of ^{95}Y has been investigated by looking for a β with end-point at 1.29 MeV (E_1) in one detector and the two γ's in two adjacent ones (E_2, E_3). In particular, we consider: i) 0.70 MeV $< E_1 <$ 1.29 MeV, ii) E_2 and E_3 inside $\pm 1\sigma$ energy windows around the photopeak positions. With these restrictions the efficiency of the process has been evaluated to be 0.65×10^{-4} of the total ^{127}I cluster decay in the studied channel.

Four events satisfying the requirements have been found; they can be ascribed to side processes. Thus, safely we consider that the number of detected events from the searched decay mode is lower than 7.99 (90% C.L.), following the procedure given in [25]. Therefore, $S < 1.23 \times 10^5$ cluster decays (90% C.L.) in the analysed exposure and

$$\tau(^{127}_{53}\mathrm{I} \rightarrow^{32}_{14}\mathrm{Si} +^{95}_{39}\mathrm{Y}) > 3.0 \times 10^{21} \ \ \mathrm{y} \quad (90\% \ \mathrm{C.L.}).$$

2.6 The channel $^{127}_{53}$I $\rightarrow$ $^{49}_{21}$Sc + $^{78}_{32}$Ge

Figure 6 shows the main part of the decay chain of $^{78}_{32}$Ge produced in the possible spontaneous cluster decay:

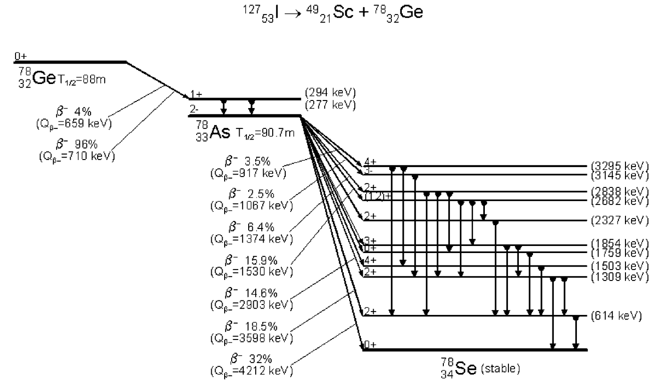

Fig. 6. Main part of the decay chain useful to understand the event pattern considered here to investigate the possible $^{127}_{53}$I $\rightarrow$ $^{49}_{21}$Sc + $^{78}_{32}$Ge cluster decay [27]. The Monte Carlo simulation for the efficiency evaluation obviously accounts for the whole decay schema of the involved isotopes.

$^{127}_{53}$I $\rightarrow$ $^{49}_{21}$Sc + $^{78}_{32}$Ge. The $^{49}_{21}$Sc decay chain is not more selective offering only γ's with low probabilities (< 0.05%).

In order to investigate this possible decay channel, we have searched for the time sequence of two events: i) the first one with multiplicity $M = 1$ (only detector a fires) and energy E_{a_1} released by the $^{49}_{21}$Sc and $^{78}_{32}$Ge fragment nuclei (Q of the process: 29.4 MeV); ii) the second one —within a time interval Δt— with multiplicity $M = 3$ given by the β-decay of the $^{78}_{33}$As (β in detector a and associated γ's in the detectors b and c); in fact, as shown in fig. 6, about 6% of the $^{78}_{33}$As β-decays are associated to two characteristic photons (1.240 MeV and 0.614 MeV).

In particular, the energy window $E_{a_1} > 5$ MeV has cautiously been considered, while the other requirements have been: i) $\Delta t < 14000$ s; ii) 1.00 MeV $< E_{a_2} <$ 2.35 MeV; iii) E_{b_2} in the energy window 0.614 MeV $\pm$ 2σ; iv) E_{c_2} in the energy window 1.240 MeV $\pm$ 2σ. As evaluated by the Monte Carlo code, these requirements allow to select $2.12 \cdot 10^{-4}$ of the total cluster decays of $^{127}_{53}$I in the studied channel.

Sixty-six events have been found satisfying the given requirements; they are fully compatible with the expected number of random coincidences: 54 ± 3. In these calculations we have suitably considered a dead time —negligible for all the other channels— due to the fact that the time sequence cannot be looked for in the last part of each data run; it is about 6%.

Thus, the 90% C.L. upper limit, $S < 1.24 \times 10^5$ cluster decays, can be derived leading to the limit:

$$\tau(^{127}_{53}\mathrm{I} \rightarrow^{49}_{21}\mathrm{Sc} +^{78}_{32}\mathrm{Ge}) > 2.8 \times 10^{21} \ \mathrm{y} \ (90\% \ \mathrm{C.L.})$$

2.7 The channel $^{127}_{53}$I $\rightarrow$ $^{48}_{20}$Ca + $^{79}_{33}$As

Figure 7 shows the main part of the decay chain of the $^{79}_{33}$As produced in the possible spontaneous cluster decay of $^{127}_{53}$I $\rightarrow^{48}_{20}$Ca + $^{79}_{33}$As. The $^{48}_{20}$Ca is not considered here since it is a quasi-stable nucleus apart from its highly forbidden β-decay and its $\beta\beta$-decay modes.

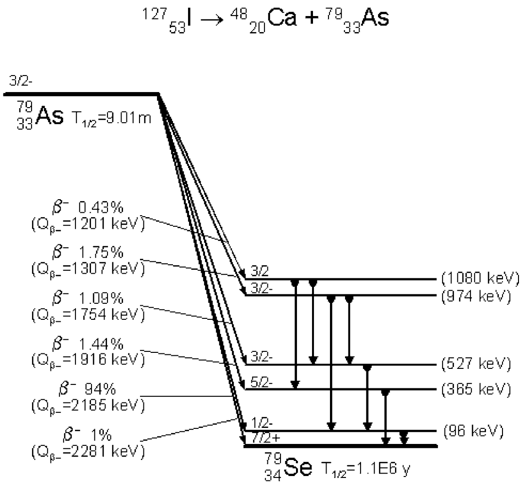

Fig. 7. Main part of the decay chain useful to understand the event pattern considered here to investigate the possible $^{127}_{53}\mathrm{I} \rightarrow {}^{48}_{20}\mathrm{Ca} + {}^{79}_{33}\mathrm{As}$ cluster decay [28]. The Monte Carlo simulation for the efficiency evaluation obviously accounts for the whole decay schema of the involved isotopes.

For each detector we have searched for an event pattern equal to that of the previous case; in particular: i) the first event with multiplicity $M = 1$ (only detector a fires) and energy E_{a_1} released by the $^{48}_{20}\mathrm{Ca}$ and $^{79}_{33}\mathrm{As}$ fragment nuclei (Q of the process: 28.9 MeV); ii) the second event —within the time interval Δt— with multiplicity $M = 2$ given by the $^{79}_{33}\mathrm{As}$ β-decay (β in the detector a and the associated γ's in the detector b). In fact, as shown in fig. 7, the $^{79}_{33}\mathrm{As}$ β-decay is associated in 1.49% of the cases to the emission of a 0.432 MeV photon and in the 1.86% of the cases to a 0.365 MeV photon.

Also in this case we cautiously considered for the first events $E_{a_1} > 5$ MeV, while the other requirements are: i) $\Delta t < 270$ s; ii) 1.00 MeV $< E_{a_2} <$ 1.85 MeV; iii) E_{b_2} in the energy window [0.365 MeV -2σ]–[0.432 MeV $+ 2\sigma$]. The detection efficiency, evaluated by the Monte Carlo code, for the given event pattern is $3.56 \cdot 10^{-4}$ of the total cluster decays of $^{127}_{53}\mathrm{I}$ in the studied channel.

In the experimental data 348 events, satisfying the selection criteria, have been found; they fully agree with the expected number of the random coincidences: 361 ± 5 events. Thus, the upper limit (90% C.L.) on the cluster decays number is $S < 5.5 \times 10^4$, which leads to the limit

$$\tau({}^{127}_{53}\mathrm{I} \rightarrow {}^{48}_{20}\mathrm{Ca} + {}^{79}_{33}\mathrm{As}) > 6.8 \times 10^{21}\ \mathrm{y}\ (90\%\ \mathrm{C.L.}).$$

3 Conclusions

The deep experimental site, the large exposure, the effective shielding of the detectors and the detectors' radiopurity have allowed to investigate possible cluster radioactivity in $^{127}\mathrm{I}$, achieving the new limits of table 1.

Further experimental efforts are foreseen on the basis of the new DAMA/LIBRA setup; moreover, other nuclides are also under considerations.

Table 1. Limits on lifetimes of possible cluster decay modes of $^{127}\mathrm{I}$ measured in the present experiment.

Process	Lower limit of the lifetime (90% C.L.) (y)
$^{127}_{53}\mathrm{I} \rightarrow {}^{30}_{12}\mathrm{Mg} + {}^{97}_{41}\mathrm{Nb}$	2.1×10^{24}
$^{127}_{53}\mathrm{I} \rightarrow {}^{34}_{14}\mathrm{Si} + {}^{93}_{39}\mathrm{Y}$	5.5×10^{22}
$^{127}_{53}\mathrm{I} \rightarrow {}^{24}_{10}\mathrm{Ne} + {}^{103}_{43}\mathrm{Tc}$	1.4×10^{23}
$^{127}_{53}\mathrm{I} \rightarrow {}^{28}_{12}\mathrm{Mg} + {}^{99}_{41}\mathrm{Nb}$	2.0×10^{22}
$^{127}_{53}\mathrm{I} \rightarrow {}^{32}_{14}\mathrm{Si} + {}^{95}_{39}\mathrm{Y}$	3.0×10^{21}
$^{127}_{53}\mathrm{I} \rightarrow {}^{49}_{21}\mathrm{Sc} + {}^{78}_{32}\mathrm{Ge}$	2.8×10^{21}
$^{127}_{53}\mathrm{I} \rightarrow {}^{48}_{20}\mathrm{Ca} + {}^{79}_{33}\mathrm{As}$	6.8×10^{21}

References

1. A. Sandulescu *et al.*, Sov. J. Part. Nucl. **11**, 528 (1980).
2. H.J. Rose, G.A. Jones, Nature **307**, 245 (1984).
3. D.V. Aleksandrov *et al.*, JETP Lett. **40**, 909 (1984).
4. R. Bonetti, A. Guglielmetti, in *Heavy Elements and Related New Phenomena*, edited by W. Greiner, R.K. Gupta, Vol. **2** (World Scientific, Singapore, 1999) p. 643.
5. S.P. Tretyakova *et al.*, Prog. Theor. Phys. Suppl. **146**, 530 (2002).
6. R. Bonetti *et al.*, Phys. Rev. C **51**, 2530 (1995).
7. D.N. Poenaru *et al.*, Phys. Rev. C **47**, 2030 (1993).
8. A. Guglielmetti *et al.*, Phys. Rev. C **56**, 2912 (1997).
9. G. Audi *et al.*, Nucl. Phys. A **729**, 337 (2003).
10. D.N. Poenaru *et al.*, At. Data Nucl. Data Tables **34**, 423 (1986).
11. D.N. Poenaru *et al.*, Phys. Rev. C **65**, 054308 (2002).
12. M. Balasubramaniam *et al.*, Phys. Rev. C **70**, 017301 (2004).
13. Z.Z. Ren *et al.*, Phys. Rev. C **70**, 034304 (2004).
14. A.Ya. Balysh *et al.*, Sov. Phys. JETP **64**, 21 (1986).
15. E. Bukhner *et al.*, Sov. J. Nucl. Phys. **52**, 193 (1990).
16. R. Bernabei *et al.*, Phys. Lett. B **424**, 195 (1998); R. Bernabei *et al.*, Phys. Lett. B **450**, 448 (1999); P. Belli *et al.*, Phys. Rev. D **61**, 023512 (2000); R. Bernabei *et al.*, Phys. Lett. B **480**, 23 (2000); R. Bernabei *et al.*, Phys. Lett. B **509**, 197 (2001); R. Bernabei *et al.*, Eur. Phys. J. C **23**, 61 (2002); P. Belli *et al.*, Phys. Rev. D **66**, 043503 (2002).
17. R. Bernabei *et al.*, Eur. Phys. J. C **18**, 283 (2000).
18. R. Bernabei *et al.*, Riv. Nuovo Cimento **26**, No. 1 (2003), astro-ph/0307403.
19. R. Bernabei *et al.*, Phys. Lett. B **408**, 439 (1997).
20. R. Bernabei *et al.*, Phys. Lett. B **389**, 757 (1996); R. Bernabei *et al.*, Nuovo Cimento A **112**, 1541 (1999); R. Bernabei *et al.*, Phys. Rev. Lett. **83**, 4918 (1999); F. Cappella *et al.*, Eur. Phys. J. direct C **14**, 1 (2002); R. Bernabei *et al.*, Phys. Lett. B **515**, 6 (2001); P. Belli *et al.*, Phys. Rev. C **60**, 065501 (1999); P. Belli *et al.*, Phys. Lett. B **460**, 236 (1999).
21. R. Bernabei *et al.*, Nuovo Cimento A **112**, 545 (1999).
22. P.M. Endt, Nucl. Phys. A **521**, 1 (1990).
23. R. Bernabei *et al.*, Phys. Lett. B **389**, 757 (1996).
24. W.R. Nelson, *et al.*, SLAC-Report-265, Stanford, 1985.
25. K. Hagiwara *et al.*, Phys. Rev. D **66**, 1 (2002).
26. T. Burrows, Nucl. Data Sheet **68**, 635 (1993).
27. S. Rab, Nucl. Data Sheet **63**, 1 (1991).
28. B. Singh, Nucl. Data Sheet **70**, 437 (1993).